Sādhanā Vol. 41, No. 7, July 2016, pp. 805–815
DOI 10.1007/s12046-016-0514-7

Combined effect of natural convection and non-gray gas radiation with partial heating

A MAZGAR[1,2,*] and F BEN NEJMA[2]

[1]The Institute of Applied Sciences and Technology of Mahdia, University of Monastir, Sidi Messaoud, 5111 Mahdia, Tunisia
[2]The Research Unit of Ionized and Reactive Media Study, The Preparatory Institute for Engineering Studies of Monastir, University of Monastir, 5019 Monastir, Tunisia
e-mail: mazgarakram@yahoo.fr

MS received 17 November 2013; revised 8 February 2016; accepted 15 April 2016

Abstract. The present paper reports numerical results of combined effects of non-gray gas radiation and natural convection between two vertical plates with partial heating at walls. The plates are symmetrical and made of two equal zones alternately isotherm and insulated. The idea is to predict that thermal radiation will attenuate the difference pre-established in the literature, between choosing a partial heating from the top and the bottom of the wall. Computations are carried out to establish flow and temperature fields of the fluid in the enclosure. The effect of enclosure dimensions and boundary conditions are analyzed. Using the computed temperature fields, the mean Nusselt number is calculated. The results show that there is no major influence of two-dimensional radiation to reduce the difference between the reported top and bottom heating for the chosen gas.

Keywords. Natural convection; partial heating; thermal radiation.

1. Introduction

Considerable attention is given to the study of natural convection in enclosures. It is of practical interest in many engineering applications, such as thermal insulation, building heating, design of heat exchangers and thermal behavior of nuclear reactor. In most of the studies dealing with buoyancy induced convection between plates, walls are considered to be isothermal, insulated or exposed to a heat flux. However, in many engineering applications like solar energy collection and cooling of electronic components, heating takes place over a narrow segment of walls, for which the buoyancy is created by the thermal gradient generated between walls. In such cases, it is very useful to know the size and the location of the heater. The active walls may be subject to abrupt temperature non-uniformities due to shading or other effects. Hence, optimum heater size and location should be determined for better utilization of such systems. Chu *et al* [1] study both theoretically and experimentally the effect of localized heating in rectangular channels using an unsteady state formulation. In this study, as one of the vertical walls is partially heated, the whole opposite vertical wall is kept at a lower temperature. A numerical investigation of natural convection of air in square cavities with half-active and half-insulated vertical wall is made by Valencia and Frederick [2]. The effects of aspect ratio and size of heat source on free convection in a discretely heated vertical cavity are investigated by Shen *et al* [3]. Refai and Yovanovich [4] perform a numerical study to examine the influence of discrete heat source location on natural convection heat transfer in a vertical square enclosure. Hasnaoui *et al* [5] present a numerical investigation of natural convection heat transfer in rectangular cavities partially heated from below, demonstrating the existence of multiple steady-state solutions and the oscillatory behavior for a given set of the governing parameters. Nicolas and Nansteel [6] experimentally analyze a study focused on the natural convection inside a square enclosure in which a portion of the lower surface is heated with a uniform heat while one vertical boundary is isothermally cooled. Yücel [7] develops a numerical model to predict the flow and heat transfer in a square enclosure with variable size heater and cooler on the vertical walls. It is claimed that for a given cooler size, the mean Nusselt number decreases with increasing the heater size. It is also shown that for a given heater size, the mean Nusselt number increases with increasing the cooler size. Results of a numerical study of buoyancy-induced flow and heat transfer in a two-dimensional square enclosure with localized heating from below and symmetrical cooling from the sides are presented by Aydin and Yang [8]. They show a raise of the average Nusselt number at the heated part of the

*For correspondence

lower wall with an increase of the Rayleigh number. The entropy generation due to the transient heat transfer and buoyancy-driven flow in a square enclosure heated partially from a vertical lateral wall and cooler isothermally from the opposite vertical wall is investigated by Berrin *et al* [9]. They find that the most active site is observed at the upper corner of the heated part of the side wall. Calcagni *et al* [10] present results of an experimental and numerical study of free convective heat transfer in a square enclosure characterized by a discrete heater located on the lower wall and cooled from the lateral walls. As expected, they show that an increase of the heat source dimension produces a raise in heat transfer particularly for high Rayleigh number. Numerical simulations of laminar, steady, two-dimensional natural convection flows in a square enclosure with discrete heat sources on the left and bottom walls are investigated by Chen and Chen [11]. It is observed that by increasing the length of heat source segment, the heat transfer rate is gradually increased. Ben Cheikh *et al* [12] perform simulations of natural convection in air-filled two-dimensional square heated for two kinds of lengths of the heat source. Their results are presented in the form of streamline and isotherm plots as well as the variation of the Nusselt number and maximum temperature at the heat source surface. Aghajani Delavar *et al* [13] investigate the effect of changing the heater location on natural convection flows and entropy generation with non-linear phenomena within enclosed rectangular cavities, showing that the location of heater has a great effect on the flow pattern and temperature fields in the enclosure and subsequently on entropy generation. A comprehensive numerical investigation on the natural convection in a rectangular enclosure due to partial heating and cooling at vertical walls is investigated by Alam *et al* [14]. They view that increasing the Rayleigh number implies the enhancement of thermal buoyancy force. As a result, the local as well as average heat transfer rate is expected to increase. It is also claimed that the local heat transfer increases as well as increases the aspect ratio. Nardini and Paroncini [15] analyze the effects of the dimensions and the positions of heating sources in the lateral walls of a square cavity to observe how the sizes and the positions of the heat sources influence the velocity field. Cianfrini *et al* [16] numerically study laminar natural convection heat transfer inside air-filled, partially heated from below and cooled at one side. They find that the heat transfer rate increases with increasing the heater size and the Rayleigh number, while it decreases with increasing the aspect ratio of the cavity. Oueslati *et al* [17] carry out a numerical study of double-diffusive natural convection in an enclosure with a partial vertical heat and mass sources for an aspect ratio four. They investigate the influence of various dimensionless parameters (Rayleigh number, buoyancy ratio, source location, Lewis number, and source length) on the flow behavior. In addition, they obtain correlations of average Nusselt and Sherwood numbers. Mahapatra *et al* [18] study natural convection in an enclosure with alternately active heat sources for different switch over time period. They assess the effects of alternating time period on heat transfer.

Thermal radiation plays an important role in heat transfer in enclosures. The majority of research works, including coupled radiation and natural convection, take only into account the effects of surface radiation. However, radiative heat transfer in participating gases cannot be neglected even at a normal temperature range. Lauriat [19] presents a study of combined radiation–convection in gray fluids, enclosed in vertical cavities. He shows that radiation decreases the intensity of the flow at low Rayleigh numbers and, in contrast, leads to increased convective regimes. Fusegi *et al* [20] study a numerical computation of interaction between natural convection and radiation in a cubical enclosure filled with a non-gray gas. Tan and Howell [21] perform a numerically analysis of combined radiation and natural convection in a two-dimensional emitting, absorbing and isotropically scattering square medium. They conclude that the presence of radiation will increase the bulk temperatures of the fluid and may have a significant influence on the fluid flow and temperature distributions. Yücel *et al* [22] numerically investigate the combined natural convection and radiation in an asymmetrically heated square enclosure, with both adiabatic and perfectly conducting end walls. They present the effects of optical thickness, scattering and wall emissivity on the flow, the temperature fields and heat transfer rates. Mesyngier and Farouk [23] report a numerical study of the turbulent natural convection-non-gray gas radiation interaction and the associated heat transfer in a square enclosure with differentially heated vertical walls and insulated horizontal walls. The enclosure is filled with a single participating gas (H_2O or CO_2) or a homogeneous mixture of two participating gases along with diluent (N_2). They propose a new correlation relating Nusselt number at the isothermal vertical walls as a function of the Rayleigh number and the optical thickness of the medium. Colomer *et al* [24] perform the phenomenon of radiation and natural convection in both transparent and participating media in a three-dimensional differentially heated cavity. They show the influences of Rayleigh and Planck numbers as well as the optical thickness. Mahapatra [25] numerically simulates the transport phenomena in steady, two-dimensional and laminar flow accompanied by heat transfer in a partially heated and partially cooled cavity in the presence of radiatively absorbing, emitting and scattering medium. Borjini *et al* [26] numerically investigate the effect of radiative heat transfer on the three-dimensional buoyancy flow in a cubic differentially heated cavity for a gray, emitting–absorbing and isotropically scattering medium. Results show that the structure of the main flow is considerably altered by the conduction–radiation parameter. Mazgar *et al* [27] conduct a numerical computation of combined radiation and natural convection in participating media through a vertical cylinder and between two

isothermal vertical plates. They show that the existence of water vapor, even in small quantities, improves the heat transfer rate and increases considerably the evacuated mass flow rate. Mondal and Mishra [28] and Mondal and Li [29] use the lattice Boltzmann method (LBM) to analyze natural convection in the presence of volumetric radiation in a square cavity containing an absorbing, emitting and scattering medium. They conclude that the effect of radiation on streamlines is more significant for higher values of Rayleigh number. However, this effect is not sensitive to the values of the scattering albedo and the extinction coefficient. Kumar and Eswaran [30] present a numerical simulation of combined radiation and natural convection in a three-dimensional differentially heated rectangular cavity. Results reveal that heat transfer decreases with the increase in optical thickness. Ben Nejma and Slimi [31] report a numerical simulation of fluid flow, heat and mass transfers by combined natural convection and radiation in a humid air bounded by isothermal vertical walls. They find that the existence of water vapor, even in small quantities, improves the heat transfer rate and increases considerably the evacuated flow rate. Lari *et al* [32] analyze the combined heat transfer of natural convection and radiation in a two-dimensional square cavity containing participating gases. The results show that even under normal room conditions with a low temperature difference, the radiation plays a significant role on temperature distribution and flow pattern in the cavity. El Ayachi *et al* [33] investigate a numerical study of natural convection and surface radiation within a square cavity filled with air and discretely heated and cooled from the four walls. Their results are presented and compared to those given in the case of pure natural convection.

The present work is intended to examine the partial heating of non-gray gas radiation due to natural convection between two vertical plates. The walls are symmetrical and made of two equal zones alternately isotherm and insulated. A numerical model is developed to predict flow and temperature fields of the fluid in the enclosure. The effect of enclosure dimensions and boundary conditions are analyzed. Calculations of the mean Nusselt number for different values of the influencing parameters are also made and discussed through this paper.

1.1 *General formulation*

The physical model under study is shown in figure 1. Humid air, considered to be an absorbing–emitting and non-gray gas, is bounded by two vertical plates with partial heating at walls. The first configuration (case 1) consists on a bottom heating system, while the second is generated by a top heating one (case 2). We note that scattering effect is neglected compared to absorbing and emission in gas radiation since the medium contains no particles. The physical properties of the medium, considered to be a perfect gas, are

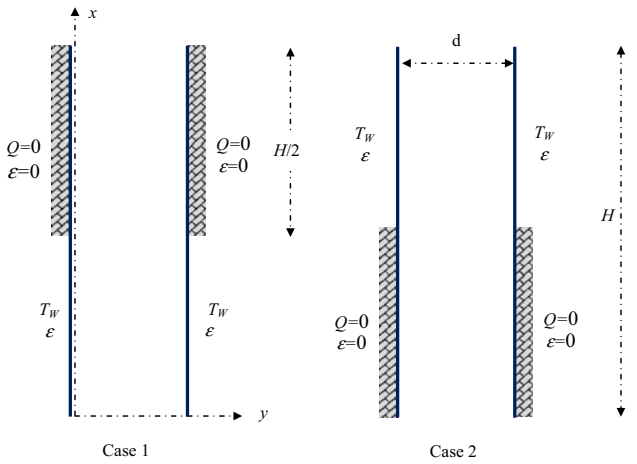

Figure 1. Geometry and boundary conditions of the physical problem.

regarded as variables and are published by Ben Nejma and Slimi [31]. The plates, made of two equal zones alternately isotherm and insulated, are symmetrical in order to avoid the reverse flow phenomenon. The thermal transfers owing to steady-state natural convection driven by buoyancy forces are described by the following conservation equations of mass, momentum and energy balance equations.

$$\frac{\partial(\rho u_x)}{\partial x}+\frac{\partial(\rho u_y)}{\partial y}=0 \tag{1}$$

$$\rho\left(u_x\frac{\partial u_x}{\partial x}+u_y\frac{\partial u_x}{\partial y}\right)=-\frac{\mathrm{d}P_m}{\mathrm{d}x}+(\rho_0-\rho)g+\frac{\partial}{\partial y}\left(\mu\frac{\partial u_x}{\partial y}\right) \tag{2}$$

$$\rho Cp\left(u_x\frac{\partial T}{\partial x}+u_y\frac{\partial T}{\partial y}\right)=\frac{\partial}{\partial y}\left(k\frac{\partial T}{\partial y}\right)-div(\vec{q}_r). \tag{3}$$

In order to calculate the spectral absorption coefficients, we have used the high-temperature spectroscopic absorption parameters given by Soufiani and Taine [34]. All of these equations [i.e. Eqs. (1)–(3)] are associated with the conservation equation of the mass flow rate on various cross-sections of the stream discharge [Eq. (4)], in order to calculate the flow rate and the dynamic pressure gradient Eq. (5), as shown by Ben Nejma and Slimi [31].

$$\dot{m}(x)=\int_0^d\rho(T(x,y))u_x(x,y)\mathrm{d}y=\rho(T_0)u_0d \tag{4}$$

$$\int_0^H\frac{\mathrm{d}P_m}{\mathrm{d}x}\cdot\mathrm{d}x={}^1\!/_2\rho(T_0)u_0^2. \tag{5}$$

In fact, the boundary condition on the dynamic pressure has a great importance in the flow rate, but very little influence on the exchange coefficient. For velocity at entry, we

choose a uniform profile which is linked with the dynamic pressure by Eq. (5).

The relevant boundary conditions associated with the present problem are summarized by the system of Eq. (6):

$$\begin{cases} u_x(x=0,y)=u_0; \quad u_x(x,y=0)=u_x(x,y=d)=0 \\ u_y(x=0,y)=0; \quad u_y(x,y=0)=u_y(x,y=d)=0 \\ T(x=0,y)=T_0 \\ case1 \begin{cases} T(x,y=0)=T(x,y=d)=T_W; \quad x\in[0,\frac{H}{2}] \\ \left.\frac{\partial T}{\partial y}\right|_{y=0}=\left.\frac{\partial T}{\partial y}\right|_{y=d}=0; \quad x\in[\frac{H}{2},H] \end{cases} \\ case2 \begin{cases} T(x,y=0)=T(x,y=d)=T_W; \quad x\in[\frac{H}{2},H] \\ \left.\frac{\partial T}{\partial y}\right|_{y=0}=\left.\frac{\partial T}{\partial y}\right|_{y=d}=0; x\in[0,\frac{H}{2}] \end{cases} \end{cases} \tag{6}$$

In addition, the radiative boundary conditions are given as follows:

For insulated walls:

$$\begin{cases} I_v^i\left(y=0,\vec{\Omega}\right) = \frac{1}{\pi}\int\limits_{\vec{\Omega}'/\vec{\Omega}'.\vec{n}<0} I_v^i\left(y=0,\vec{\Omega}'\right).\xi\left(\vec{\Omega}'\right)\mathrm{d}\Omega' \\ I_v^i\left(y=d,\vec{\Omega}\right) = \frac{1}{\pi}\int\limits_{\vec{\Omega}'/\vec{\Omega}'.\vec{n}<0} I_v^i\left(y=d,\vec{\Omega}'\right).\xi\left(\vec{\Omega}'\right)\mathrm{d}\Omega'. \end{cases} \tag{7}$$

For isothermal walls:

$$\begin{cases} I_v^i\left(y=0,\vec{\Omega}\right) = \varepsilon.I_v^b(T_W)+\frac{1-\varepsilon}{\pi}\int\limits_{\vec{\Omega}'/\vec{\Omega}'.\vec{n}<0} I_v^i\left(y=0,\vec{\Omega}'\right).\xi\left(\vec{\Omega}'\right)\mathrm{d}\Omega' \\ I_v^i\left(y=d,\vec{\Omega}\right) = \varepsilon.I_v^b(T_W)+\frac{1-\varepsilon}{\pi}\int\limits_{\vec{\Omega}'/\vec{\Omega}'.\vec{n}<0} I_v^i\left(y=d,\vec{\Omega}'\right).\xi\left(\vec{\Omega}'\right)\mathrm{d}\Omega'. \end{cases} \tag{8}$$

It is worth noting that the duct's inlet and outlet are assumed to be like fictitious black walls at T_0 temperature.

We note that for entry (300 K, 1 atm), the saturation pressure given by Rankin's formula is slightly lower at 3500 Pa. Therefore, the water vapor molar fraction should not exceed 3%.

The expressions of the local conductive and radiative Nusselt numbers along the vertical walls are given as follows:

$$Nu_c(x)=\frac{-d}{(T_W-T_0)}\left(\frac{\partial T(x,y)}{\partial y}\right)_{y=0} \tag{9}$$

$$Nu_r(x)=\frac{1}{2k(T_W)}\frac{d}{(T_W-T_0)}\int_0^d div(\vec{q}_r(x,y))\mathrm{d}y. \tag{10}$$

The global Nusselt number is defined as follows:

$$Nu_g(x)=Nu_c(x)+Nu_r(x). \tag{11}$$

The mean Nusselt number over the duct is given by Eq. (12):

$$Nu_m=\frac{1}{H}\int_0^H (Nu_c(x)+Nu_r(x)).\mathrm{d}y. \tag{12}$$

2. Numerical solution procedure

The numerical procedure applied for integrating the governing equations of the fluid flow is based on the finite volume method using an upwind scheme through axial direction and a centred difference scheme through traverse direction. The non-linear differential equations were solved using the damping Newton method. In order to resolve the radiative transfer equation Eq. (13) and to predict the spectral nature of thermal radiation, we applied the discrete ordinates method (DOM) through S_4 directions, in association with the Statistical Narrow Band Correlated-k (SNBCK) model [35, 36], using the 4-point Gauss–Lobatto quadrature where the gas radiative properties are represented by four non-gray mediums at each non-overlapping band. It can be noted that the use of the S_4 quadrature seems to be sufficient [37–39].

$$\frac{\mathrm{d}I_v^i(l,\vec{\Omega})}{\mathrm{d}l}=-\kappa_v^i(l).I_v^i(l,\vec{\Omega})+\kappa_v^i(l).I_v^0(T). \tag{13}$$

This equation will give the expression of the radiative source term as shown by Sakly *et al* [40]:

$$div(\vec{q}_r)=\sum_{bands}\int_{4\pi}\sum_{i=1}^{4} w^i.\kappa_v^i\left(I_v^0-I_v^i\left(\vec{\Omega}\right)\right)\mathrm{d}\Omega\Delta v. \tag{14}$$

In order to transform the differential equations into algebraic forms, they are integrated over the finite control volumes. The use of a mixed grid system defined by 200 uniform nodes through transverse direction and 300 Tchebychev's sinusoidal nodes through axial direction

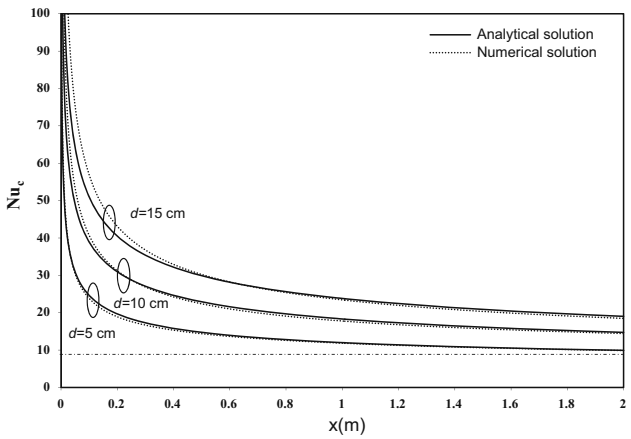

Figure 2. Validation of the model [$u_0 = 0.1$ m/s, $T_0 = 400$ K, $T_W = 600$ K, $P = 1$ atm (at constant physical properties)].

seems to be reasonable for accuracy and computational economy [31]. The utilization of a sinusoidal grid following axis direction is essential to take into account the strong variation of the dynamic pressure gradient. This is important for calculating the flow rate and precisely for estimating the exchanges in the entrance vicinities of the duct.

The validation of our numerical model is done by comparing the local Nusselt number calculated through forced convection configuration considering the physical properties as constant, with that provided through the analytic solution [41]. Figure 2 shows that the difference is very weak

3. Results and discussion

A selected set of graphical results are presented in figures 3–15 to provide an easy understanding of the influence of thermal radiation and boundary conditions on heat transfer. Although radiation is not the dominating factor in the total exchanges because of the weak water content in the air, it has a great importance on flow rate. Figure 3 shows the temperature profiles in case of heating from the bottom (case 1) and heating from the top (case 2). We note that important temperature gradients are developed in the vicinity of heated walls and there is no symmetry in temperature profiles, between choosing a partial heating from the top of the wall and a partial heating from the bottom. Graphics of the radiative source term given in figure 4, mention an asymmetry in the profile distributions between partial heating from the top and the bottom of the duct. This can be explained by the dominance of natural convection on thermal radiation effect, due to low vapor content in the air. Figure 5 illustrates the profiles of global Nusselt number, with and without thermal radiation, in the two initially preset configurations. We can remark that the conductive Nusselt numbers present decreasing profiles which are practically similar to the trends of the global Nusselt numbers. Otherwise, we can clearly distinguish the effect of thermal conduction on Nusselt profiles, in the form of a marked discontinuity observed at the mid-length, which represents the boundary between heated and insulated walls. We can also note in the profiles of figure 6, the influence of the 2d radiation exchange effect on the fluid flow by the appearance of low values of radiative Nusselt number respectively, in vicinities of the second half of the duct (case 1) and in vicinities of the first half of the duct (case 2). This slightly contributes to the reduction of the discontinuity caused by the thermal conduction. We notice in the case 1 configuration of this last figure a remarkable increasing of the radiative Nusselt number in the inlet

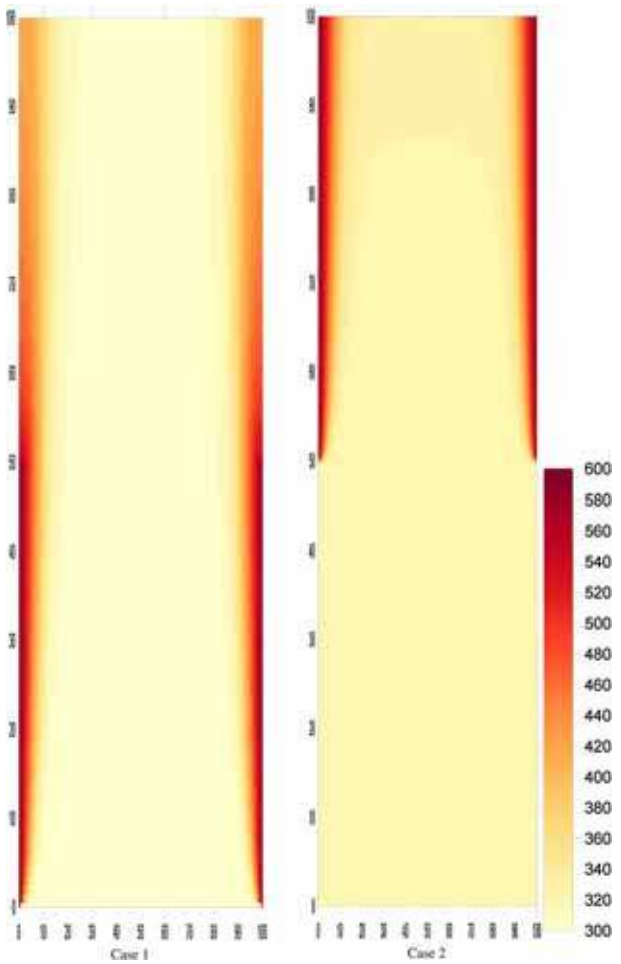

Figure 3. Temperature profiles (°K) ($d = 0.1$ m, $H = 4$ m, $T_0 = 300$ K, $T_W = 600$ K, $x_{H2O} = 0.02$, $\varepsilon = 1$).

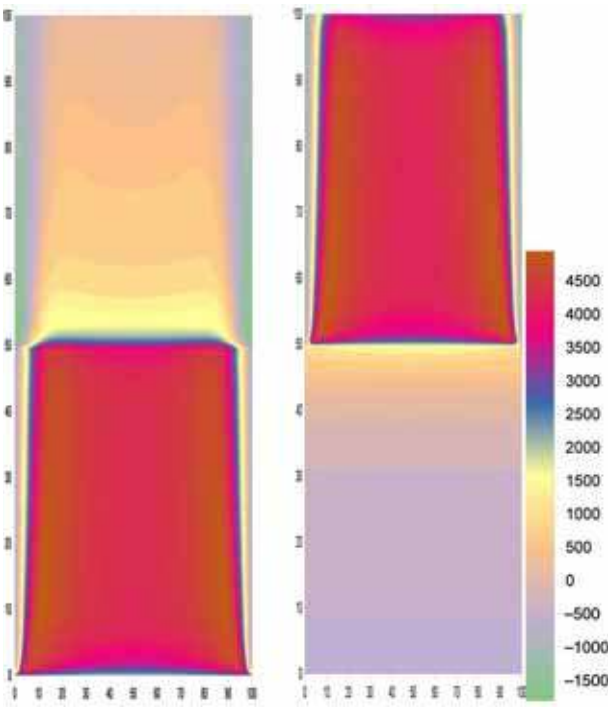

Figure 4. Radiative source term profiles (W/m^3) ($d = 0.1$ m, $H = 4$ m, $T_0 = 300$ K, $T_W = 600$ K, $x_{H2O} = 0.02$, $\varepsilon = 1$).

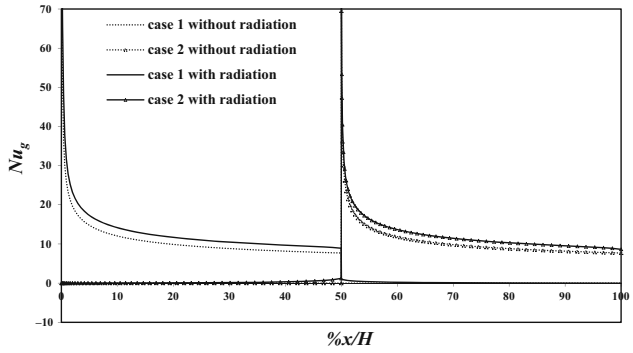

Figure 5. Global Nusselt profiles ($d = 0.1$ m, $H = 4$ m, $T_0 = 300$ K, $T_W = 600$ K, $x_{H2O} = 0.02$, $\varepsilon = 1$).

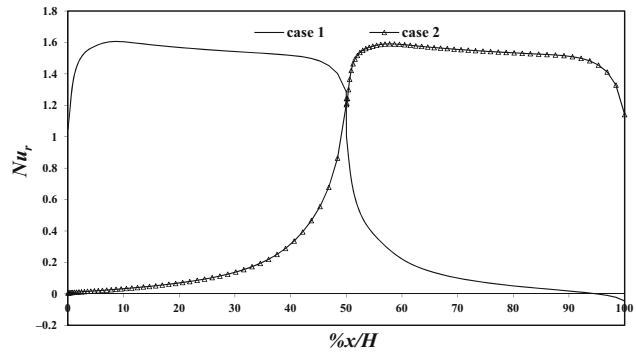

Figure 6. Local radiative Nusselt profiles ($d = 0.1$ m, $H = 4$ m, $T_0 = 300$ K, $T_W = 600$ K, $x_{H2O} = 0.02$, $\varepsilon = 1$).

section. A reverse phenomenon occurs in the case 2 configuration with a strong decreasing of radiative Nusselt number at the outlet section. These large changes in the radiative Nusselt number at the inlet and the outlet sections of the duct are due to the thermal exchanges with the external cold environment. Figures 7–10 present the effect of thermal radiation on flow rate, for varied boundary conditions. We can show in figure 7 the profiles of the mean Nusselt number and the inlet velocity as a function of the channel length. It can be noted in figure 7a, that thermal radiation seems to add a constant component to the Nusselt number values calculated without taking into account the radiative effect. A remarkable difference can be observed in figure 7b between the flow rate calculated with and without radiation. This difference is accentuated with the rise of the duct length. Bearing in mind the wall temperature effect on the flow rate profiles (figure 8), we can say that taking into account the radiation effect, the mean Nusselt number profiles (figure 8a) are practically uniform. However, in absence of thermal radiation, these profiles tend to have slightly decreasing trends when rising the wall temperature. Otherwise, it is important to signal that the difference signaled between the values of the mean Nusselt number in the two initially preset configurations (case 1 and case 2) is attenuated when increasing the wall temperature. Referred

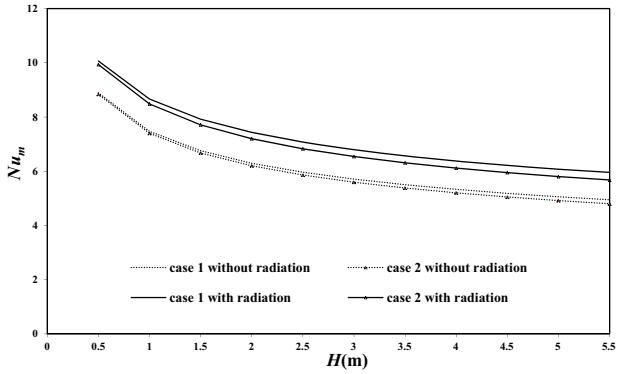

(a)

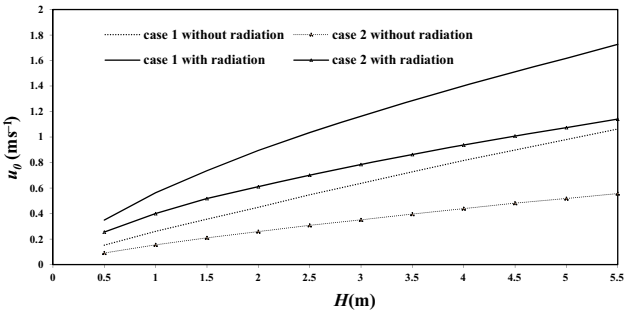

(b)

Figure 7. Effect of the duct's length ($d = 0.1$ m, $T_0 = 300$ K, $T_W = 600$ K, $x_{H2O} = 0.02$, $\varepsilon = 1$).

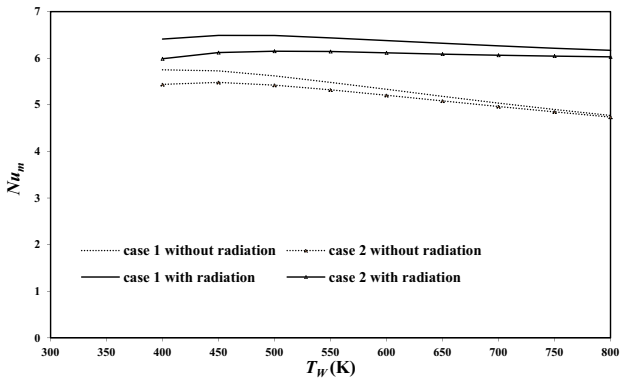

(a)

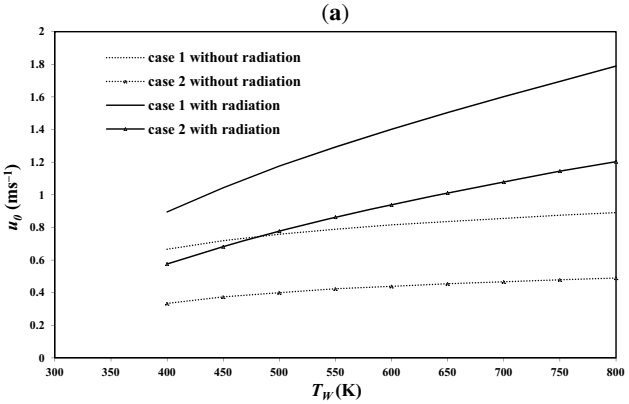

(b)

Figure 8. Effect of the wall temperature ($d = 0.1$ m, $H = 4$ m, $T_0 = 300$ K, $x_{H2O} = 0.02$, $\varepsilon = 1$).

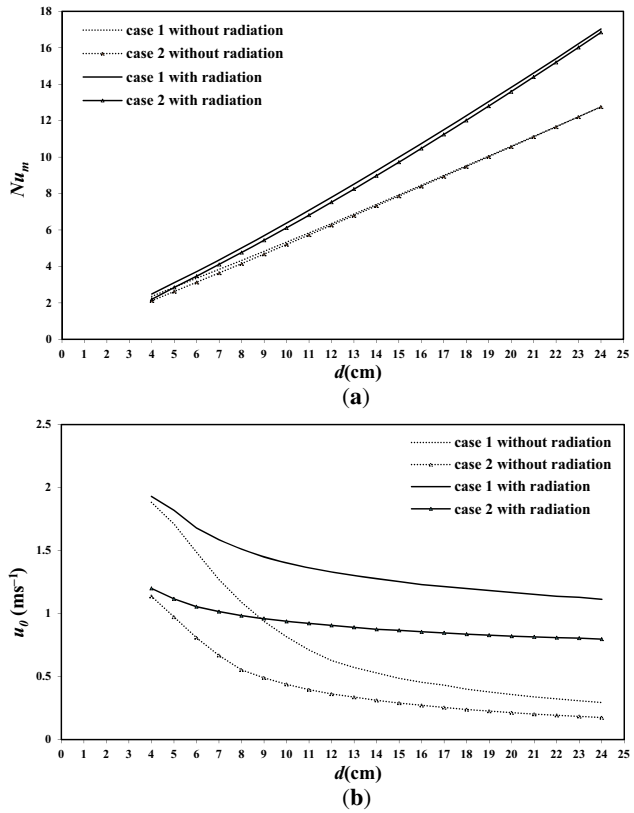

Figure 9. Effect of the duct's width ($H = 4$ m, $T_0 = 300$ K, $T_W = 600$ K, $x_{H2O} = 0.02$, $\varepsilon = 1$).

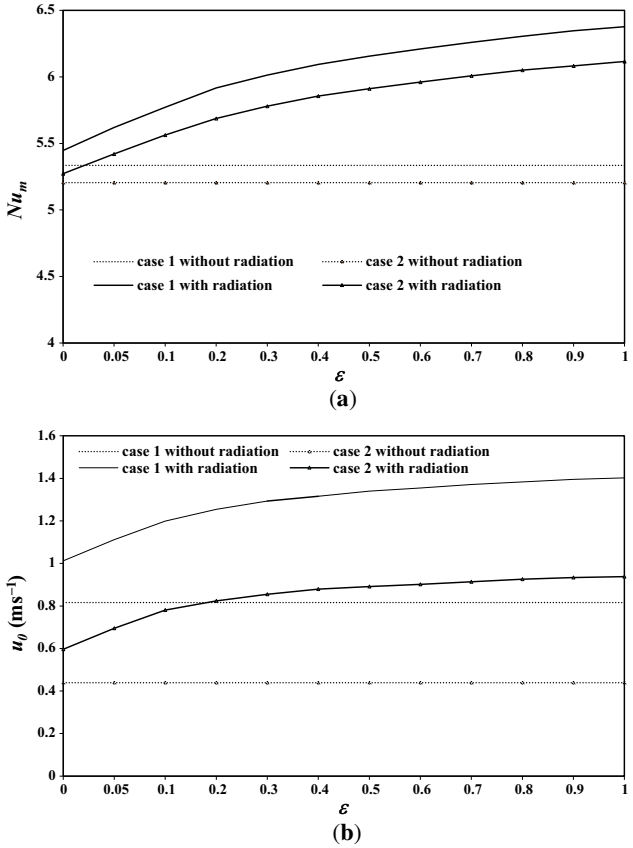

Figure 10. Effect of the wall emissivity ($d = 0.1$ m $H = 4$ m, $T_0 = 300$ K, $T_W = 600$ K, $x_{H2O} = 0.02$).

to figure 8b, we must report the significant enhancement in the inlet velocity profiles if thermal radiation is taken into account. In this case, the difference that exists between case 1 flow rate profiles and those of case 2 diminishes when decreasing the wall temperature. However, this difference remains unchanged in absence of thermal radiation. Profiles plotted in figure 9 exhibit the variations of the average Nusselt number and the inlet velocity for different duct's widths. Figure 9a shows that when thermal radiation is taken into account, the mean Nusselt numbers are approaching exponential profiles. However, these trends are practically linear if thermal radiation is not taken into consideration. In addition, increasing the duct's width, results in rise in the difference between the mean Nusselt numbers, calculated by considering the radiative effect and that given in absence of radiation. The flow rate velocity profiles are affected by the duct width as seen in figure 9b. In fact, the inlet velocity decreases rapidly as the duct width increases, and progressively, this diminishing is attenuated to have practically horizontal profiles, because of the reduced interaction between plates for higher widths. Computations results using different values of emissivity are presented in figure 10. We note that emissivity does not affect the difference between the values of the mean Nusselt number, calculated in both of the two initially preset configurations. This is being the same for the inlet velocity

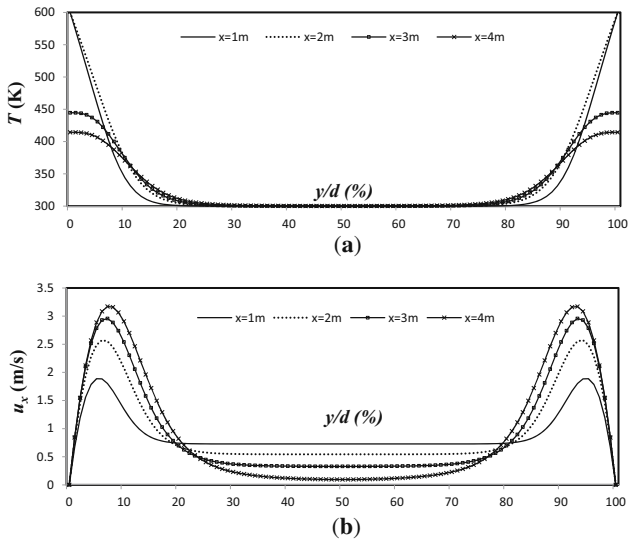

Figure 11. Temperature and axial velocity (case 1 without radiation: $d = 0.1$ m, $H = 4$ m, $T_0 = 300$ K, $T_W = 600$ K, $x_{H2O} = 0.02$, $\varepsilon = 1$).

profiles and can be explained by the fact that radiosity of the *i*th element of the enclosure is practically reduced to the radiosity of the black body walls, since the medium is optically thin.

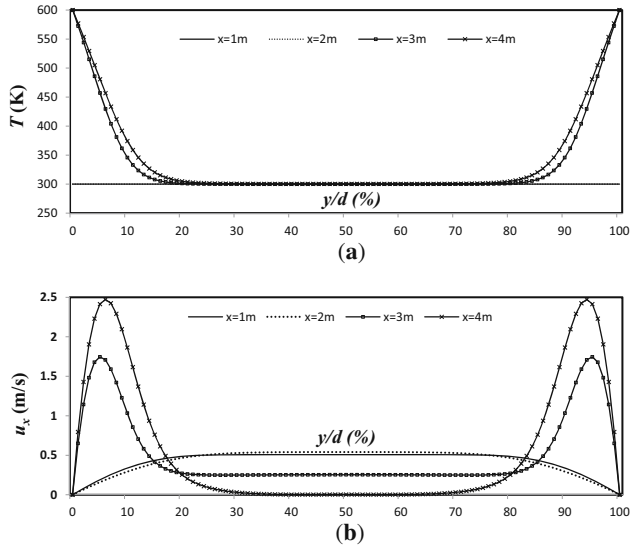

Figure 12. Temperature and axial velocity (case 2 without radiation: $d = 0.1$ m, $H = 4$ m, $T_0 = 300$ K, $T_W = 600$ K, $x_{H2O} = 0.02$, $\varepsilon = 1$).

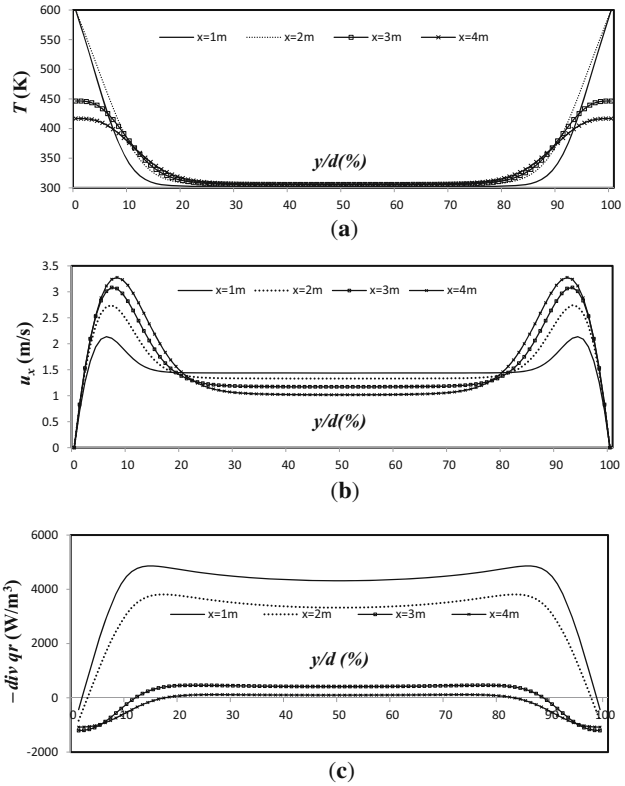

Figure 13. Temperature, axial velocity and radiative source term (case 1 with radiation: $d = 0.1$ m, $H = 4$ m, $T_0 = 300$ K, $T_W = 600$ K, $x_{H2O} = 0.02$, $\varepsilon = 1$).

Bearing figure 11a in mind, we note that for the first part of the duct, the medium is subjected to a remarkably heating in the vicinities of the walls due to the presence of strong gradients temperature. Moreover, there is no thermal heating for the advanced streamwise locations situated at the second part of the duct, with less important temperature gradients, uniformizing the temperature profile.

A close look to figure 11b permits to remark that due to buoyancy forces, the heated fluid particles are strongly aspirated in the vicinities of walls, with axial velocity maxima that progressively increase and move away from the walls as well as advancing through the axial direction. This aspiration of the fluid particles reduces the fluid flow in the central zone of the flow. In (case 2) configuration (figure 12), we can signal the absence of heat transfers in the first half of the duct, resulting in the establishment of dynamic flow stabilization, evolving towards a Poiseuille flow. In the second half of the duct, heating occurs with the appearance of temperature gradients and the aspiration of fluid particles in vicinities of walls due to buoyancy effect. The effects of thermal radiation on temperature, axial velocity and the radiative source term are established in figure 13 and figure 14 for case 1 and case 2, respectively. We can report a weak radiative effect on the temperature profiles with non-major influence of two-dimensional thermal radiation especially for low aspect ratio. However, a big impact is shown on the axial velocity profiles, especially in the central zone of the flow, where buoyancy forces are practically identical since the medium remains optically thin, providing the same acceleration of the fluid particles and masking the viscosity effect. The source term profiles of figure 13c present negative values in vicinities of walls since the gas temperature is high and the fluid particles exchange thermal radiation with the central zone of the flow. By moving away from the plates, the radiative source term becomes positive and remains practically uniform by the fact that the medium is optically thin. The corresponding values of the radiative source term are attenuated as well as advancing through the axial direction while remaining in the first half of the duct. In the second half, the radiative source term presents lower profiles reflecting gas-gas thermal radiation exchanges. These trends are progressively attenuated as well as the temperature profile becomes uniform. It can be remarked by examining the radiative source term curves of figure 14c, that due to the weak aspect ratio (d/H), radiative heat transfer is quasi absent in the entire first half of the duct. Thermal radiation starts to be noticeable as well as we approach the second half of the duct, there where the view factor with which the gas observes the second section is equal to 0.5. In the second half of the duct, we notice similar profiles to those reported in the first half of (case 1) configuration.

Graphics given in figure 15, establish the profiles of the local maximum values of the Reynolds number over wall normal coordinate. The shown high values of the Reynolds number dispute the assumption of a laminar flow, although they remain local values. The fact that the debited velocity is uncontrollable and conditioned by the aspiration phenomena may cause such findings. In order to sidestep this problem, it is preferable to choice an

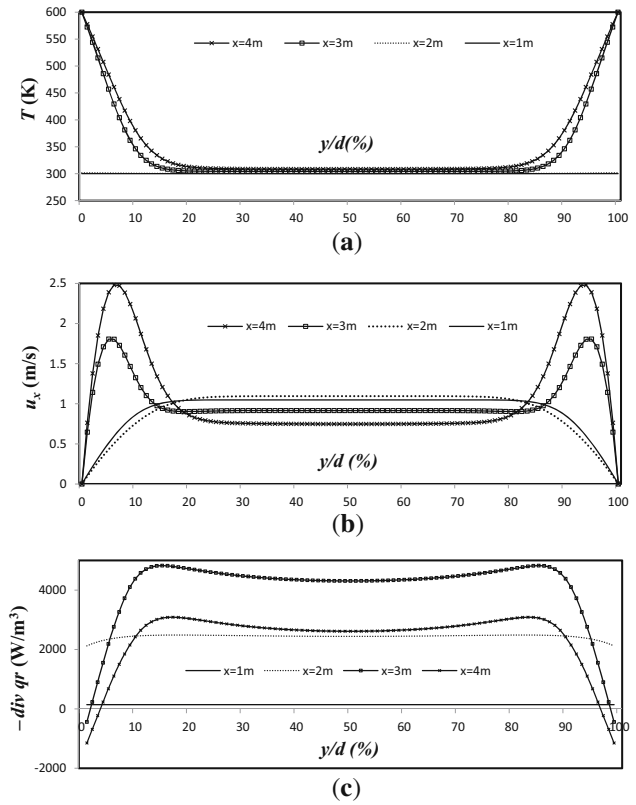

Figure 14. Temperature, axial velocity and radiative source term (case 2 with radiation $d = 0.1$ m, $H = 4$ m, $T_0 = 300$ K, $T_W = 600$ K, $x_{H2O} = 0.02$, $\varepsilon = 1$).

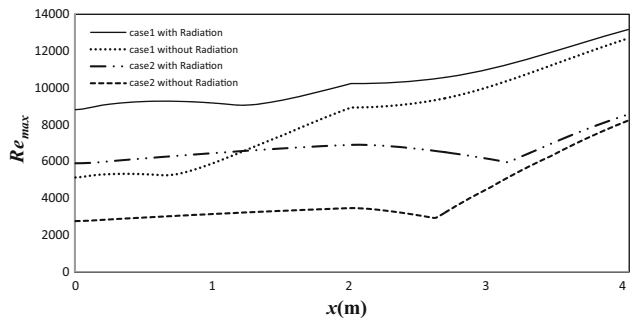

Figure 15. Local maximum Reynolds number ($d = 0.1$ m, $H = 4$ m, $T_0 = 300$ K, $T_W = 600$ K, $x_{H2O} = 0.02$, $\varepsilon = 1$).

enclosure with a reduced height while using not very high working temperatures.

4. Conclusion

In this paper, the numerical calculation of partial heating due to combined thermal radiation and natural convection in participating media is investigated. This study is focused on a laminar flow of temperature-dependent and non-gray gas bounded by two vertical plates. An association between the discrete ordinates method through S_4 directions and the $SNBCK_4$ model is used to solve the radiation part of the problem. Computations are carried out to predict flow and temperature fields in the enclosure. The effect of enclosure dimensions and boundary conditions are analyzed. Based on the results, radiative effect considerably affects both of heat transfer rate and flow rate. It slightly contributes to the reduction of discontinuity caused by thermal conduction. In addition, the two-dimensional radiation attenuation of the difference between heating from the top and heating from the down of the duct is less important than expected because of the low vapor content in the air. This work can reflect an appropriate physical approach by choosing a reduced height enclosure while using not very high working temperatures, for the purpose of avoiding the turbulence effect.

Nomenclature

Cp	Specific heat capacity at constant pressure (J kg^{-1} K^{-1})
d	Width of plates (m)
g	Gravitational acceleration (m s^{-2})
H	Height of plates (m)
I	Radiative intensity (W m^{-2} sr^{-1})
k	Thermal conductivity (W m^{-1} K^{-1})
l	Optical path (m)
$\dot{m}$	Mass flow rate (kg m^{-1} s^{-1})
Nu	Nusselt number
P	Pressure (Pa)
Pm	Dynamic pressure (Pa)
Q	Heat exchange (J)
q	Heat flux density (W m^{-2})
Re_y	Local algebraic wall normal Reynolds number $Re = \frac{\rho.d.u_x}{\mu}$
T	Temperature (K)
u	Velocity (m s^{-1})
w	Weight parameter
x,y	Cartesian coordinates

Greek symbols

ε	Wall emissivity
κ	Absorption coefficient (m^{-1})
ρ	Density (kg m^{-3})
μ	Dynamic viscosity (N s m^{-2})
Δv	Spectral resolution (cm^{-1})
$\vec{\Omega}$	Ray direction
$d\Omega$	Elementary solid angle around $\vec{\Omega}$

Subscripts

0	Inlet
m	Mean
W	Wall
v	Spectral
x	Along x-axis
y	Along y-axis

c Conductive
r Radiative
g Global

Superscripts

i Partial non-gray medium
0 Black body

References

[1] Chu H H S, Churchill S W and Patterson C V S 1976 The effect of heater size, location, aspect ratio and boundary conditions on two-dimensional laminar natural convection rectangular channels. *ASME J. Heat Transf.* 98(2): 194–201

[2] Valencia A and Frederick R L 1989 Heat transfer in square cavities with partially active vertical walls. *Int. J. Heat Mass Transf.* 32(8): 1567–1574

[3] Shen R, Prasad V and Keyhani M 1989 Effect of aspect ratio and size of heat source on free convection in a discretely heated vertical cavity. *ASME, Heat Trans. Division* 121: 45–54

[4] Refai A G and Yovanovich M M 1991 Influence of discrete heat source location on natural convection heat transfer in a vertical square enclosure. *ASME J. Electron. Packaging* 113(3): 268–274

[5] Hasnaoui M, Bilgen E and Vasseour P 1992 Natural convection heat transfer in rectangular cavities partially heated from below. *J. Thermophys. Heat Transf.* 6(2): 255–264

[6] Nicolas J D and Nansteel M W 1993 Natural convection in a rectangular enclosure with partial heating of the lower surface: experimental results. *Int. J. Heat Mass Transf.* 36(16): 4067–4071

[7] Yücel N 1994 Natural convection in rectangular enclosures with partial heating and cooling. *Wärme-und Stoffübertragung* 29(8): 471–477

[8] Aydin O and Yang W J 2000 Natural convection in enclosures with localized heating from below and symmetrical cooling from sides. *Int. J. Numer. Method. Heat Fluid Flow* 10(5): 518–529

[9] Berrin Erbay L, Altaç Z and Sülüs B 2004 Entropy generation in a square enclosure with partial heating from a vertical lateral wall. *Heat Mass Transf.* 40(12): 909–918

[10] Calcagni B, Marsili F and Paroncini M 2005 Natural convective heat transfer in square enclosures heated from below. *Appl. Therm. Eng.* 25(16): 2522–2531

[11] Chen T H and Chen L Y 2007 Study of buoyancy-induced flows subjected to partially heated sources on the left and bottom walls in a square enclosure. *Int. J. Therm. Sci.* 46(12): 1219–1231

[12] Ben Cheikh N, Ben Beya B and Lili T 2007 Influence of thermal boundary conditions on natural convection in a square enclosure partially heated from below. *Int. Commun. Heat Mass Tranf.* 34(3): 369–379

[13] Aghajani Delavar M, Farhadi M and Sedighi K 2011 Effect of discrete heater at the vertical wall of the cavity over the heat transfer and entropy generation using lattice Boltzmann method. *Therm. Sci.* 15(2): 423–435

[14] Alam P, Kumar A, Kapoor S and Ansari S R 2012 Numerical investigation of natural convection in a rectangular enclosure due to partial heating and cooling at vertical walls. *Commun. Nonlinear Sci. Numer. Simu.* 17(6): 2403–2414

[15] Nardini G and Paroncini M 2012 Heat transfer experiment on natural convection in a square cavity with discrete sources. *Heat Mass Transf.* 48(11): 1855–1865

[16] Cianfrini C, Corcione M, Habib E and Quintino A 2013 Convective transport in rectangular cavities partially heated at the bottom and cooled at one side. *J. Therm. Sci.* 22(1): 55–63

[17] Oueslati F, Ben-Beya B and Lili T 2014 Numerical investigation of thermosolutal natural convection in a rectangular enclosure of an aspect ratio four with heat and solute sources. *Heat Mass Transfer* 50(5): 721–736

[18] Mahapatra P S, Manna N K, Ghosh K and Mukhopadhyay A 2015 Heat transfer assessment of an alternately active bi-heater undergoing transient natural convection. *Int. J. Heat Mass Transf.* 83: 450–464

[19] Lauriat G 1982 Combined Radiation-Convection in gray fluids enclosed in vertical cavities. *J. Heat Transf.* 104(4): 609–615

[20] Fusegi T, Ishii K, Farouk B and Kuwahara K 1991 Natural convection-radiation interactions in a cube with a non-gray gas. *Numer. Heat Transf. A-Appl.* 19(2): 207–217

[21] Tan Z and Howell J R 1991 Combined radiation and natural convection in a two-dimensional participating square medium. *Int. J. Heat Mass Transf.* 34(3): 785–793

[22] Yücel A, Acharya S and Williams M L 1994 Natural convection of a radiating fluid in a square enclosure with perfectly conducting end walls. *Sadhana* 19(5): 751–764

[23] Mesyngier C and Farouk B 1996 Turbulent natural convection-non-gray gas radiation analysis in a square enclosure. *Numer. Heat Transf. A-Appl.* 29(7): 671–687

[24] Colomer G, Costa M, Consul R and Oliva A 2004 Three-dimensional numerical simulation of convection and radiation in a differentially heated cavity using the discrete ordinates method. *Int. J. Heat Mass Transf.* 47(2): 257–269

[25] Mahapatra S K 2008 Numerical simulation for optimal configuration of heater and cooler locations with natural convection inside a square enclosure and the effect of radiation in the presence of radiatively active medium. *Proc. Inst. Mech. Eng. Part C J. Mech. Ing. Sci.* 222(8): 1505–1514

[26] Borjini M N, Ben Aissia H, Halouani K and Zeghmati B 2008 Effect of radiative heat transfer on the three-dimensional buoyancy flow in cubic enclosure heated from the side. *Int. J. Heat Fluid Flow* 29(1): 107–118

[27] Mazgar A, Ben Nejma F and Charrada K 2009 Entropy generation through combined non-grey gas radiation and natural convection in vertical pipe. *Prog. Comput. Fluid Dyn.* 9(8): 495–506

[28] Mondal B and Mishra S C 2009 Simulation of natural convection in the presence of volumetric radiation using the lattice Boltzmann method. *Numer. Heat Transf. A-Appl.* 55(1): 18–41

[29] Mondal B and Li X 2010 Effect of volumetric radiation on natural convection in a square cavity using lattice Boltzmann method with non-uniform lattices. *Int. J. Heat Mass Transf.* 53: 4935–4948

[30] Kumar P and Eswaran V 2010 A numerical simulation of combined radiation and natural convection in a differential heated cubic cavity. *J. Heat Transf.* 132(2), 1–13.

[31] Ben Nejma F and Slimi K 2010 Combined natural convection and radiation in humid air bounded by isothermal vertical walls. *High Temp. High Press.* 39(3): 217–226

[32] Lari K, Baneshi M, Gandjalikhan Nassab S A, Komiya A and Maruyama S 2011 Combined heat transfer of radiation and natural convection in a square cavity containing participating gases. *Int. J. Heat Mass Transf.* 54: 5087–5099

[33] El Ayachi R, Raji A, Hasnaoui M, Abdelbaki A and Naïmi M 2011 Combined effects of radiation and natural convection in a square cavity submitted to cross gradients of temperature: Case of partial heating and cooling. *Comput. Therm. Sci.* 3(1): 73–87

[34] Soufiani A and Taine J 1997 High temperature gas radiative property parameters of statistical narrow-band model for H_2O, CO_2 and CO, and correlated-k model for H_2O and CO_2. *Int. J. Heat Mass Transf.* 40(4): 757–991

[35] Ben Nejma F, Mazgar A and Charrada K 2008 Entropy generation through combined non-grey gas radiation and forced convection between two parallel plates. *Energy* 33(7): 1169–1178

[36] Mazgar A, Ben Nejma F and Charrada K 2013 Second law analysis of coupled mixed convection and non-grey gas radiation within a cylindrical annulus. *Int. J. Math. Model. Methods Appl. Sci.* 7(3): 265–276

[37] Ben Nejma F, Mazgar A and Charrada K 2010a Radiative entropy generation in a cylindrical enclosure. In: *Eur. Conf. Chem. Eng. ECCE'10, Eur. Conf. Civil Eng., ECCIE'10, Eur. Conf. Mech. Eng., ECME'10, Eur. Conf. Control, ECC'10*, 67–70

[38] Ben Nejma F, Mazgar A and Charrada K 2010b Volumetric and wall non grey gas entropy creation in a cylindrical enclosure. *WSEAS Trans. Heat Mass Transf.* 5(4): 217–226

[39] Ben Nejma F, Mazgar A and Charrada K 2011 Application of the statistical narrow-band correlated-k model to entropy generation through non-grey gas radiation inside a spherical enclosure. *Int. J. Exergy* 8(2): 128–147

[40] Sakly A, Mazgar A and Ben Nejma F 2015 Thermal radiation contribution on humidification process in a cylindrical annular duct. *High Temp.-High Press.* 44(3): 163–186

[41] Taine J and Petit J P 1989 *Transferts thermiques: mécanique des fluides anisothermes*. Paris: Edition Bordas